*Chinese Journal of*
**POLYMER SCIENCE**

RESEARCH ARTICLE

https://doi.org/10.1007/s10118-026-3658-x
*Chinese J. Polym. Sci.* **2026**, *44*, 2681–2690

# Facile Construction of Hierarchical Polymeric Positive Temperature Coefficient Composites for Improved Reproducibility

Bao-Yu Wang[a,†], Heng-Yu Zhao[a,†], Xin Ji[b], Wei Hu[a], Yu-Ru Duan[b], Jian-Ze Li[b], Zi-Hao Zhang[b], Ying Liang[b*], Bin Fang[b], and Zhen Zhang[b*]

[a] *School of Materials Science and Engineering, East China University of Science and Technology, Shanghai 200237, China*
[b] *School of Physics, East China University of Science and Technology, Shanghai 200237, China*

Electronic Supplementary Information

**Abstract** Adopting composite matrices has great significance for improving the performance of polymeric positive temperature coefficient (PPTC) materials. However, the uncontrollable selective distribution of fillers in different matrices induced by the differences in compatibility severely limits the flexible design and regulation of conductive networks. A solution-mixing strategy based on the solubility difference of polymer matrices in different solvents was employed to flexibly fabricate hierarchical PPTC composites, achieving the precise localization of conductive fillers. In the hierarchical structure, PVDF/TiC served as the first-level PTC material, whereas the PA1010/TiC particles acted as the other-level PTC material. The PA1010/TiC particles serving as relay stations also participated in the construction of the PVDF/TiC conductive network. Benefiting from the restriction effect of the PA1010/TiC particles for the PVDF chains and TiC fillers, the negative temperature coefficient (NTC) effect was effectively suppressed, and a maximum $I_{PTC}$ of 8.9 was obtained. Moreover, in cyclic testing, the PVDF phase crystallized posterior to the PA1010 phase, generating compression and releasing latent heat for the PA1010 phase, which synergistically reinforced the crystallization of the PA1010 phase, enabling rapid reconstruction of long-range conductive networks in the entire system. Therefore, the reproducibility and $I_{hold}$ of the hierarchical PPTC thermistor were significantly improved. This strategy not only breaks the bottleneck of the selective distribution of fillers in the multi-matrix of PPTC materials, but also achieves dynamic control of hierarchical conductive networks, suggesting a new pathway toward the overall improvement of the performance of PPTC thermistors.

**Keywords** Polymeric positive temperature coefficient thermistor; Solution mixing method; Hierarchical conductive networks; Reproducibility

**Citation:** Wang, B. Y.; Zhao, H. Y.; Ji, X.; Hu, W.; Duan, Y. R.; Li, J. Z.; Zhang, Z. H.; Liang, Y.; Fang, B.; Zhang, Z. Facile construction of hierarchical polymeric positive temperature coefficient composites for improved reproducibility. *Chinese J. Polym. Sci.* **2026**, *44*, 2681–2690.

## INTRODUCTION

PTC materials exhibit non-linear temperature-resistivity features, whose resistivity increases sharply by more than several orders of magnitude once exceeding the switch temperature ($T_s$).[1–4] The unique conductivity behavior of PTC materials, which serve as resettable protectors, has led to their extensive application in portable electronics, micromotor, and automotive battery protections.[5–8] These materials can effectively prevent damage caused by overcurrent and overtemperature resulting from shortcircuit or overload. PTC materials can be classified into two main categories: ceramic PTC (CPTC) and polymeric PTC (PPTC). While CPTC devices demonstrate exceptional performance in high-power and high-temperature environments, their susceptibility to rupture or fracture under mechanical stress or impact is attributed to the inherent brittleness of the ceramic matrix.[9–11] Additionally, the challenges associated with the high sintering temperature contribute to difficulties in the formation and processing of CPTC devices, resulting in higher manufacturing costs.[12,13]

PPTC materials are preferred in consumer electronics and mass production because of their lightweight nature, low resistance, high PTC intensity ($I_{PTC}$), and cost-effectiveness.[14–18] PPTC materials are conductive polymer composites that are fabricated by mixing crystalline polymer and conductive fillers. The PTC effect is generally believed that the conductive networks were broken during heating, owing to the thermal expansion of the polymer and the change in the distance between the conductive fillers.[15,19] The resistivity reached a peak at the melting temperature ($T_m$) or glass transition temperature ($T_g$) of the polymer. If the PPTC material is further heated after the PTC peak, a NTC effect would be observed because of the re-aggregation of the conductive particles in the molten polymer matrix.[20,21] Meanwhile, the poor compatibility between the polymer matrix and filler results in irreversible thermal movement and phase separation.[15] Thus,

* Corresponding authors, E-mail: yliang@ecust.edu.cn (Y.L.)
E-mail: zhangzhen@ecust.edu.cn (Z.Z.)
† These authors contributed equally to this work.
Received January 16, 2026; Accepted March 11, 2026; Published online May 26, 2026

along with thermal cycling, the reproducibility of the conductivity behavior is very poor.

Thus, enhancing the cycling stability of PPTC thermistors is crucial. Various strategies have been investigated to mitigate the NTC effect and improve the reproducibility of temperature-resistivity.[15,19] The poor cycling stability of the PPTC thermistor is mainly attributed to the crystallization of the polymer matrix.[22] The primary strategy to solve this problem is crosslinking the polymer matrix or adopting hybrid polymer matrices.[23–27] For instance, electron beams have been applied in the radiation crosslinking of LDPE/CB composites, and the NTC effect was weakened because the crosslinking network of the polymer restricted the migration of CB fillers.[28] In addition, dual polymer matrices of HDPE and PVDF were explored. Owing to the immiscible blending of polymers, abundant segregated structures are formed. Improved reproducibility of the PTC effect was obtained because of the strengthening crystallization of PVDF induced by the compression effect of HDPE.[29] Furthermore, by controlling the localization of the hybrid fillers in immiscible polymer blends, 3D conductive networks were constructed to significantly enhance the performance of the PPTC composites. Although studies have demonstrated that multi-matrix blending could improve the reproducibility of PPTC materials, flexible regulation of the composition of the multi-matrix blending system is challenging.[30] Because of the difference in compatibility, the selective distribution of conductive fillers in different polymer matrices is inevitable,[31–33] which significantly limits the preparation of multi-matrix PPTC materials with flexible design and regulation of conductive networks.

In this study, a solution-mixing method was proposed to design and fabricate hierarchical PPTC materials with a double-level PTC structure and performance. Therefore, the selective distribution of conductive fillers in different polymer matrices was effectively inhibited by using the solubility difference of the polymer matrices in various solvents. First, PA1010/TiC particles were fabricated using a good solvent of PA1010. Then, PA1010/TiC particles and TiC micropowders, serving as different-level fillers, were evenly dispersed in the PVDF matrix using a good solvent of PVDF, which is a non-solvent of PA1010. A double-level conductive network of (PA1010/TiC)/PVDF/TiC was constructed, in which PVDF/TiC served as the first-level PTC material, and PA1010/TiC served as the other-level PTC material. Once the circuits of the double-level PTC materials were cut off, the conductive network of PA1010/TiC crystallized ahead, which was further compressed by the delayed crystallization of the PVDF/TiC phase. Meanwhile, the latent heat released from the crystallization of the PVDF/TiC phase refined the crystallization of the PA1010 matrix. In these hierarchical structures, the PA1010/TiC phases serving as relay stations favor the formation of long-range conductive pathways, and the overall conductive networks of double-level PTC materials could be rapidly rebuilt. Therefore, the reproducibility improved and the NTC effect was suppressed. This work not only circumvents the issue of selective distribution of conductive fillers but also achieves the goal of flexibly controlling the composition of multi-matrix PPTC composite materials, thereby offering a new possibility to enhance the overall performance of PPTC thermistors.

## EXPERIMENTAL

### Materials

All the chemicals and materials were purchased and used as received. Polydecamethylene sebacamide (PA1010, DuPont11, $\rho$=1.04 g/cm$^3$, $T_m$=205 °C) was purchased from DuPont Co., Ltd. Polyvinylidene fluoride (PVDF, FR903, $\rho$=1.48 g/cm$^3$, $T_m$=168 °C) was purchased from Shanghai Huayi Sanaifu New Materials Co., Ltd. Titanium carbide (TiC with an average diameter of approximately 2.3 μm) was purchased from Qinhuangdao Yinuo High-Tech Materials Development Co., Ltd. *N*,*N*-dimethylformamide (DMF, AR) and formic acid (FA, 99%) were purchased from Sinopharm Chemical Reagent Co., Ltd. Copper foil was purchased from Shanghai Likai Material Technology Co., Ltd.

### Preparation of PA1010/TiC Particles

In a typical experiment, 2.0 g of PA1010 was dissolved in formic acid (8.0 mL) at 75 °C under magnetic stirring (150 r/min) for 30 min. After PA1010 was completely dissolved, 36.0 g of TiC micropowder was added to a formic acid solution of PA1010 (the mass ratio of PA1010 to TiC was 1:18). The mixture was stirred for 30 min to complete the pre-mixing process. Planetary ball milling was performed at 1200 r/min for 4 min using a planetary mixer (ZYMC-200V, Suzhou ZYE Precision Technology Co., Ltd.) to ensure complete dispersion. A well-mixed PA1010/TiC/formic acid dispersion was coated onto a glass substrate using a spreader with a gap of 0.30 mm. The coated glass substrate was dried at 80 °C for 120 min and 120 °C for 60 min, sequentially. After the solvent was completely evaporated, the PA1010/TiC composite sample was peeled off and ground into PA1010/TiC particles using a mortar. The PA1010/TiC particles were then sieved through a screen mesh (300 mesh) to obtain PA1010/TiC particles with a size of less than 50 μm.

### Preparation of Dispersion of PPTC Composite

0.77 g of PVDF was dissolved in 4.0 mL of DMF (which is good solvent for PVDF, non-solvent for PA1010) at 75 °C under magnetic stirring (150 r/min) for 30 min. After PVDF was completely dissolved, 9.23 g of TiC micropowder was added to the DMF solution of PVDF (the mass ratio of PVDF to TiC was 1:12). The mixture was stirred for 30 min to obtain a pre-mixed PVDF/TiC/DMF dispersion. The as-prepared 2.0 g of PA1010/TiC particles was added to the dispersion, which was magnetically stirred for 30 min. The (PA1010/TiC)/PVDF/TiC/DMF composite dispersion was ball milled on a planetary mixer at 1200 r/min for 4 min to ensure complete dispersion. In addition, different mass ratios of (PA1010/TiC) to (PVDF/TiC) were investigated. The experimental procedures are summarized in Table S1 (in the electronic supplementary information, ESI).

### Preparation of Hierarchical PPTC Thermistor

A homogeneous (PA1010/TiC)/PVDF/TiC/DMF dispersion was coated onto the rough surface of the copper foil using a spreader with a gap of 0.30 mm. The coated copper foil was dried at 80 °C for 120 min and 150 °C for 60 min, sequentially. After the complete evaporation of the solvent, the coated copper foil was folded, and the PPTC composites were stuck in the middle. Heat pressing was performed at 205 °C and 15 MPa for 20 min to fuse the layers of PPTC composite. The three-layer structure consisted of two electrode layers of copper foil and a layer of PPTC composite. The three-layer sample was die-cut into 3 mm × 4

https://doi.org/10.1007/s10118-026-3658-x

mm hierarchical PPTC thermistors. To improve the crystallinity of polymer matrix, the PPTC thermistors were heat-treated at 180 °C for 30 min and naturally cooled to room temperature in a vacuum oven.

## Characterizations

The morphology was characterized using a Phenom Nano G2 field-emission scanning electron microscope (SEM) operating at 10.0 kV. Differential scanning calorimetry (DSC) was conducted at a heating rate of 10 °C·min$^{-1}$ in a $N_2$ atmosphere (DSC Q2000, TA Instruments). Polarized optical microscopy (POM) observations were performed using a Leica DM4P microscope at 200× magnification, with a heating and cooling rate of 10 °C·min$^{-1}$ across a temperature range of 25–250 °C. To conveniently test the electrical characteristics, the wires were soldered on both surfaces of the PPTC thermistor.

### *The measurement of resistivity-temperature (ρ-T) curves and $I_{PTC}$*

The resistivity-temperature behavior of PPTC thermistor was measured by employing a high precision DC resistance tester (RK2514, Shenzhen Meiruike Electronic Technology Co., Ltd.), and the samples were heated and cooled at a rate of 3 °C·min$^{-1}$. $\rho$ was calculated using Eq. (1):

$$\rho = R \times l \times w/(d - 2h) \quad (1)$$

where $R$ is the tested resistance at different temperature (Ω); $l$, $w$, $d$ are the length, width and thickness of PPTC thermistor (cm), respectively; $h$ is the thickness of copper foil (cm).

The room-temperature resistivity ($\rho_0$) was calculated by substituting the room-temperature resistance ($R_0$) into Eq. (1). $T_s$ was extracted from the lg($\rho$)–$T$ curve, which is the temperature at which the resistance surges sharply.

And the $I_{PTC}$ was calculated using Eq. (2):

$$I_{PTC} = \lg(\rho_{max}/\rho_0) \quad (2)$$

where $\rho_{max}$ is the maximum resistivity of PPTC thermistor under heat treatment.

Five parallel measurements were performed for samples under the same experimental condition. Error bars in the figure denote the standard deviation (SD) of these five parallel measurements.

### *The measurement of hold current ($I_{hold}$)*

The PTC effect induced by an applied voltage was investigated by measuring the voltage–current (*V-I*) characteristics, and $I_{hold}$ was obtained from the *V-I* curve. A DC-regulated power supply (RPS3030D-2, Shenzhen Meiruike Electronic Technology Co., Ltd.) was used, and the applied voltages and corresponding currents were recorded. Additionally, cyclic measurements of *V-I* were performed to examine the stability of the PPTC thermistor.

## RESULTS AND DISCUSSION

For PPTC materials with dual matrices, the distribution of conductive fillers in different polymer matrices is a critical factor in determining PTC performance. However, achieving controllable localization of conductive fillers during the fabrication and service of dual-matrix PPTC materials remains challenging. As shown in Fig. 1, a solution-mixing method based on the solubility difference of polymer matrices in different solvents was employed to fabricate hierarchical PPTC composite materials. First, TiC micropowder with an average diameter of 2.3 μm (Fig. S1 in ESI) were dispersed in a formic acid solution of PA1010 through a planetary ball-milling technique, and the dispersion was further dried and ground into PA1010/TiC particles. PA1010/TiC

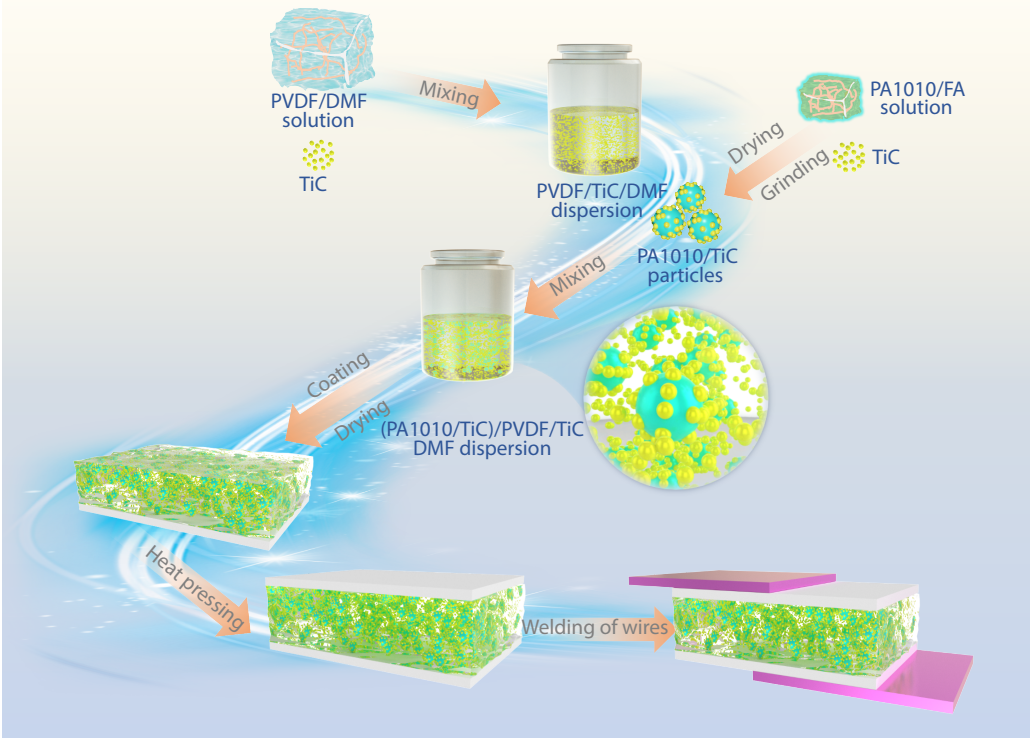


**Fig. 1** The schematic illustration of preparation route of hierarchical PPTC thermistor through using solution mixing method.

particles with an average size of approximately 30.7 μm were obtained, and TiC micropowders were well dispersed in the PA1010 matrix (Fig. S2 in ESI), owing to the good solubility of PA1010 in formic acid. Next, the PA1010/TiC particles and TiC micropowders were used as hierarchical conductive fillers and dispersed into the PVDF matrix using DMF, which is a good solvent for PVDF but a non-solvent for PA1010. Thus, the PA1010/TiC particles maintain their morphology, thereby preventing the leakage of TiC fillers from the PA1010 matrix. The (PA1010/TiC)/PVDF/TiC/DMF composite dispersion was obtained and spread on copper foil. After solvent evaporation, the coated copper foil was folded and heat-pressed. A thermistor with hierarchical structures of PA1010/TiC and PVDF/TiC was obtained, which would benefit the construction of dual-level conductive networks.

As shown in Fig. 2, the (PA1010/TiC)/PVDF/TiC composite exhibited hierarchical structures, which contained large-sized PA1010/TiC particles and small-sized TiC fillers dispersed in the PVDF matrix. With an increase in the mass ratio of PA1010/TiC to PVDF/TiC ($m_{(PA1010/TiC)}$:$m_{(PVDF/TiC)}$) from 1:5 to 4:5, the areal number density of the PA1010/TiC particles dispersed in the PVDF matrix gradually increased, and the average interparticle distance gradually decreased (Table S2 in ESI). When the PA1010/TiC particles were absent, the PVDF/TiC composites did not exhibit hierarchical structures, and only TiC fillers were homogeneously dispersed in the PVDF matrix (Fig. S3 in ESI). It should be noted that the loading concentration of TiC in the PA1010 matrix was 18:1, which was higher than that of TiC in the PVDF matrix (12:1). Therefore, the content and distribution of the conductive fillers in different polymer matrices can be precisely controlled. Hierarchical PPTC composites with PVDF/TiC served as the first-level PTC material, and PA1010/TiC served as the other-level PTC material were successfully constructed.

## PTC Properties of (PA1010/TiC)/PVDF/TiC Hierarchical Composites

As an important measurement for characterizing PTC properties, the resistivity-temperature behavior was carefully investigated by measuring the $\rho$-$T$ curves of different thermistors. As shown in Fig. 3(a), with an increase in temperature, the thermistor of PVDF/TiC composite exhibited a typical PTC phenomenon, where $\rho$ underwent slowly increased when the temperature under 155 °C ($T_s$) and then rapid growth, which was

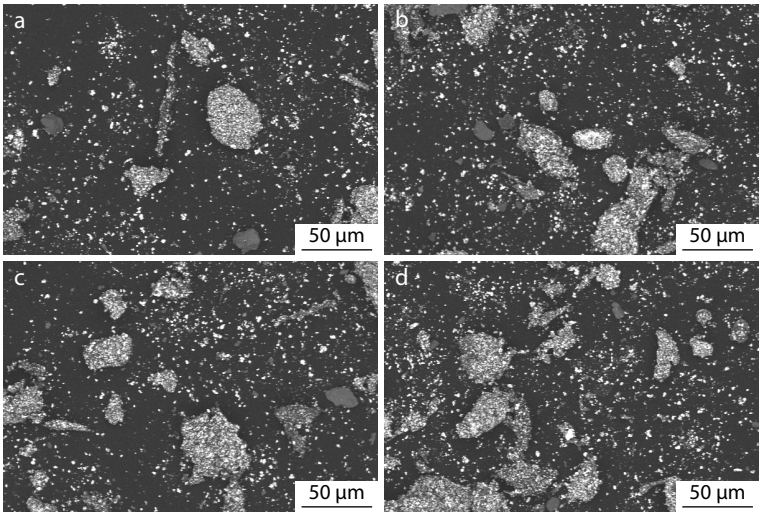


**Fig. 2** The SEM images of (PA1010/TiC)/PVDF/TiC composites with different ratios of $m_{(PA1010/TiC)}$: $m_{(PVDF/TiC)}$: (a) 1:5, (b) 2:5, (c) 3:5, (d) 4:5.

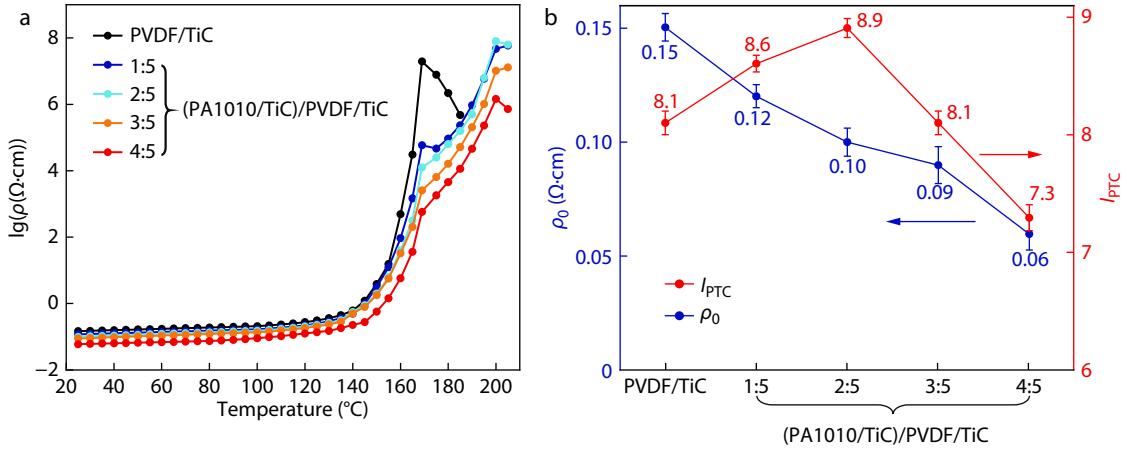


**Fig. 3** (a) The resistivity-temperature (lg($\rho$)-$T$) curves; (b) Room temperature resistivity ($\rho_0$) and PTC intensity ($I_{PTC}$) of PVDF/TiC PPTC thermistor and the hierarchical PPTC thermistors with different ratios of $m_{(PA1010/TiC)}$:$m_{(PVDF/TiC)}$.

https://doi.org/10.1007/s10118-026-3658-x

mainly attributed to breakdown of interconnected TiC networks resulting from volumetric expansion of PVDF matrix during the heating process. When the $\rho$ climbed to the top ($\rho_{max}$) at approximately 169 °C, the NTC effect appeared and the $\rho$ began to decline, which attributed to the re-agglomeration of TiC fillers bringing about the reconstruction of conductive paths at the melting temperature of PVDF matrix (172.8 °C, Fig. S4 in ESI). In contrast, with the addition of PA1010/TiC particles, the thermistors of (PA1010/TiC)/PVDF/TiC composites with different $m_{(PA1010/TiC)}$:$m_{(PVDF/TiC)}$ ratios exhibited dual PTC characteristics, the NTC effect did not appear at 200 °C. After experiencing the first transition region at approximately 170 °C, the $\rho$ further increased to its maximum ($\rho_{max}$) at approximately 200 °C. After the second transition region appeared, the trend of the rapid growth of $\rho$ disappeared, and the growth of $\rho$ became gradual, even when $\rho$ started to decrease as the mass ratio of PA1010/TiC to PVDF/TiC increased to 4:5. Compared with the single-matrix thermistor of PVDF/TiC, the hierarchical thermistors of (PA1010/TiC)/PVDF/TiC demonstrated elevated maximum resistivity temperatures, and the NTC effect was effectively suppressed. It may be speculated that the addition of PA1010/TiC particles could effectively restrict chain mobility of PVDF and TiC fillers due to the high melting point of PA1010 (201.0 °C, Fig. S4 in ESI). The NTC effect began to appear until the temperature increased to the melting point of PA1010, which was consistent with the experimental results of the $\rho$–$T$ curves.

Moreover, the $I_{PTC}$ of different thermistors were further studied, which is an important parameter for the cutting-off current capability of the PPTC thermistor and is determined by $\rho_{max}$ and $\rho_0$ ($I_{PTC}$ = lg($\rho_{max}$/$\rho_0$)). In Fig. 3(b), the $\rho_0$ of PVDF/TiC thermistor was approximately 0.15 Ω·cm. Along with the increase in the PA1010/TiC particle content, $\rho_0$ decreased approximately linearly. The lowest $\rho_0$ of 0.06 Ω·cm was obtained with the $m_{(PA1010/TiC)}$:$m_{(PVDF/TiC)}$ ratio of 4:5. The addition of PA1010/TiC particles could improve the conductivity of the hierarchical (PA1010/TiC)/PVDF/TiC composites, owing to the PA1010 matrix with a higher content of TiC fillers. Therefore, $\rho_0$ of the thermistors steadily decreased as the PA1010/TiC content gradually increased. The $I_{PTC}$ of the PVDF/TiC thermistor is approximately 8.1. When the PA1010/TiC particles were added, the $I_{PTC}$ steadily increased to 8.6 and 8.9 with the $m_{(PA1010/TiC)}$:$m_{(PVDF/TiC)}$ of 1:5 and 2:5, respectively. However, the $I_{PTC}$ of thermistors with mass ratios of 3:5 and 4:5 dropped to 8.1 and 7.3, respectively. The difference in the change trend of the $I_{PTC}$ can be attributed to variations in $\rho_0$ and $\rho_{max}$. As $\rho_0$ gradually decreases, $I_{PTC}$ initially increases. However, if the content of the highly conductive PA1010/TiC particles further increases, $\rho_{max}$ starts to decline. This is mainly because the conductive networks were constructed by PA1010/TiC particles with a higher loading level of TiC than the PVDF matrix, which was difficult to be destroyed. In addition, with the increase in the content of PA1010/TiC particles, the primary component of the conductive networks changed from TiC in the PVDF matrix to PA1010/TiC particles. The probability of reconstructing the conductive path increased because of the high content of conductive fillers in the system during the heating process. Therefore, the suitable usage of PA1010/TiC particles, serving as the other-level PTC material, could not only suppress the NTC effect, but also improve the $I_{PTC}$.

## Effect of the Hierarchical Structure on the Reproducibility

Good reproducibility is critical for an ideal PPTC material, which affects its practical applications. The $\rho$–$T$ curves of the different thermistors were cyclically measured to study reproducibility. The thermistor was naturally cooled to room temperature between the two measurements. In Fig. S5 (in ESI), the $\rho$-$T$ curves of the single-matrix PVDF/TiC thermistor overlapped within three cycles of testing, indicating the good reproducibility of thermal cycling. However, an obvious shift appeared in the fifth cycle, and the $T_s$ decreased from 155 °C to 140 °C within 20 cyclic measurements (Table S3 in ESI). Meanwhile, $\rho_0$ gradually increased, and $I_{PTC}$ decreased in a fluctuating manner during thermal cycling. This indicates that the reproducibility of the PVDF/TiC thermistor is poor.

When the PA1010/TiC particles served as other-level PTC material, the cyclic measurements of the (PA1010/TiC)/PVDF/TiC thermistors were conducted. As shown in Fig. 4, the shift in $\rho$–$T$ curves of hierarchical PPTC thermistor ($m_{(PA1010/TiC)}$:$m_{(PVDF/TiC)}$ = 1:5) within 20 cyclic measurements became narrow, and the $T_s$ gradually increased from 160 °C to 170 °C. However, the $I_{PTC}$ also decreased in a fluctuating manner, which indicated that the reproducibility was improved, but not obviously. As $m_{(PA1010/TiC)}$:$m_{(PVDF/TiC)}$ increased to 2:5, the $\rho$-$T$ curves approximately overlapped. Moreover, the $T_s$ stabilized at 165 °C. Although there was a slight decline, the $I_{PTC}$ was consistently higher than 8.0. These results demonstrate that the reproducibility of the hierarchical PPTC thermistor ($m_{(PA1010/TiC)}$:$m_{(PVDF/TiC)}$ = 2:5) is markedly improved. When $m_{(PA1010/TiC)}$: $m_{(PVDF/TiC)}$ was further increased to 3:5, the performance of the hierarchical PPTC thermistor was similar to that of $m_{(PA1010/TiC)}$:$m_{(PVDF/TiC)}$ = 1:5. The $\rho$-$T$ curves represent small-scale shifts during 20 cyclic measurements. And the $T_s$ and $I_{PTC}$ have experienced certain fluctuations, reaching 165 °C and 7.8, respectively. When the mass ratio of PA1010/TiC to PVDF/TiC was further improved to 4:5, the reproducibility significantly decreased. The shift of the $\rho$-$T$ curves broadened during 20 cyclic measurements. Moreover, the $T_s$ and $I_{PTC}$ rapidly decreased to 160 °C and 4.9, respectively. Therefore, the reproducibility of the hierarchical PPTC thermistor gradually increased and then decreased with increasing $m_{(PA1010/TiC)}$:$m_{(PVDF/TiC)}$. The minimum relative fluctuation percentages of $T_s$ and $I_{PTC}$ appeared in the hierarchical PPTC thermistor with an $m_{(PA1010/TiC)}$:$m_{(PVDF/TiC)}$ ratio of 2:5 (Table S4 in ESI). The reproducibility of the hierarchical PPTC thermistor was superior to that of reported PPTC devices (Table S5 in ESI).

Based on the experimental results, a dynamic conduction mechanism for hierarchical PPTC thermistors is proposed. As shown in Fig. 5, double-level conductive networks were formed inside the hierarchical PPTC composites, which consisted of a conductive network of PA1010/TiC particles and a conductive network of TiC micropowders dispersed in PVDF. The PA1010/TiC particles participated in the construction of the PVDF/TiC conductive network. Along with the increase in temperature, the thermal expansion of the PVDF matrix would lead to the destruction of the PVDF/TiC conductive network owing to the increase in the distance between the

https://doi.org/10.1007/s10118-026-3658-x

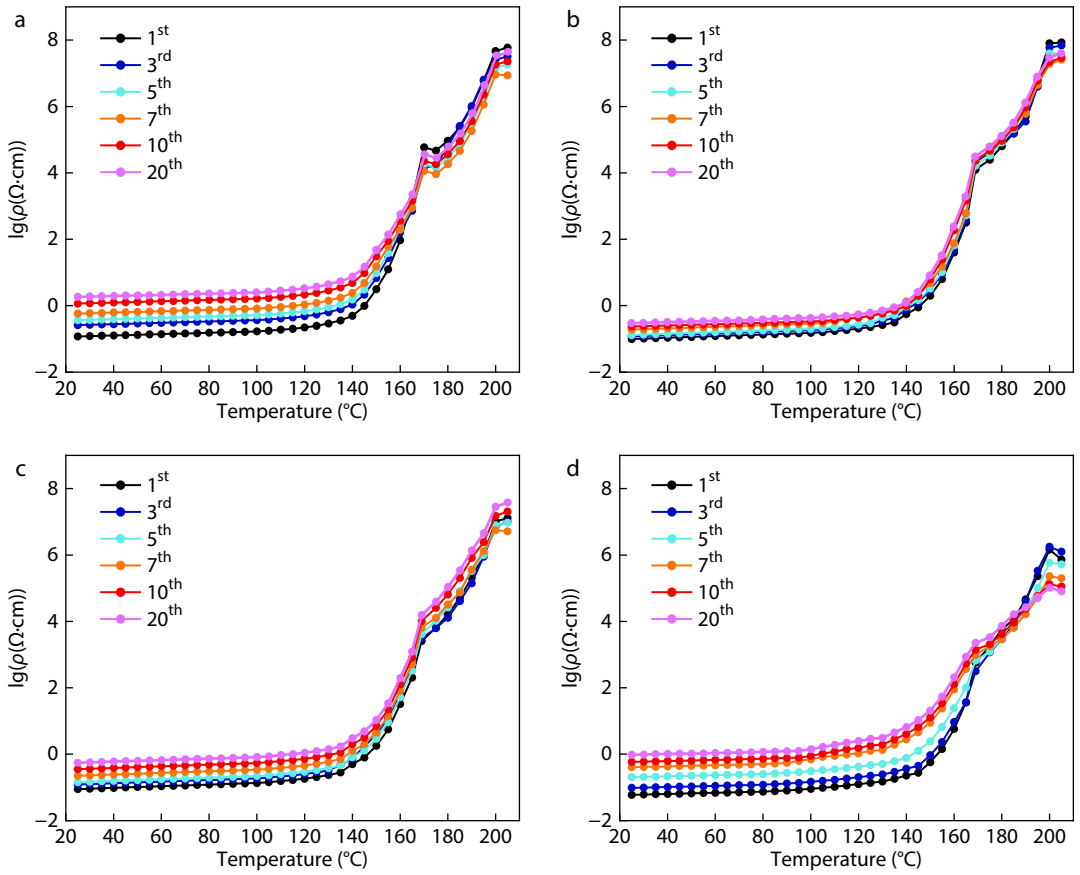


**Fig. 4** The resistivity–temperature (lg($\rho$)–$T$) curves of hierarchical PPTC thermistors of (PA1010/TiC)/PVDF/TiC with different ratios of $m_{(PA1010/TiC)}$ to $m_{(PVDF/TiC)}$ : (a) 1:5, (b) 2:5, (c) 3:5, (d) 4:5 under different number of cycles.

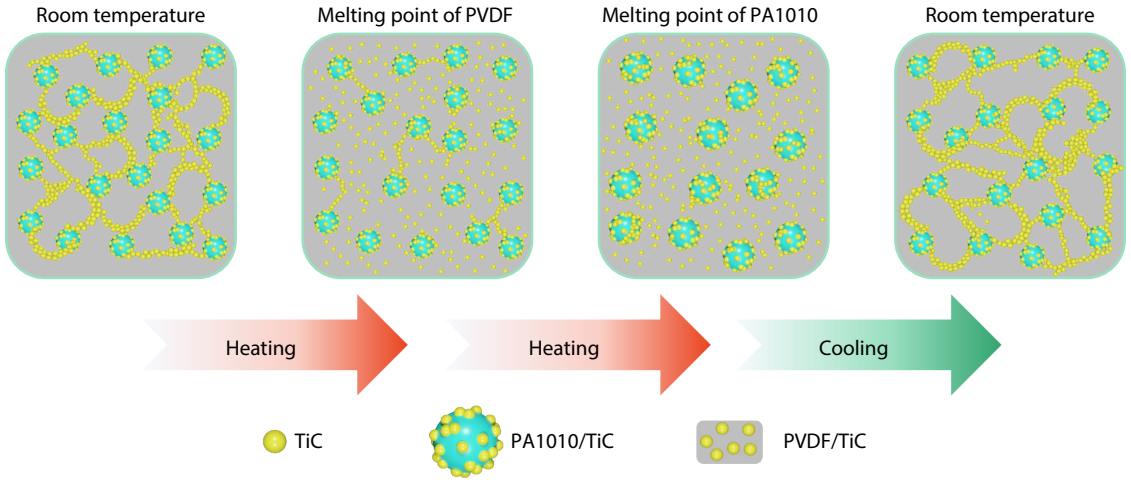


**Fig. 5** The schematic illustration of the reconstruction of hierarchical conductive network and conductive mechanism for PPTC thermistor of (PA1010/TiC)/PVDF/TiC.

conductive fillers. Thus, the resistivity of the entire system increased. Until the temperature was close to melting point of PA1010, the localized conductive network of PA1010/TiC was also destroyed. This means that the overall conductive networks were completely destroyed and $\rho$ climbed to the top ($\rho_{max}$). During the cooling process, the PA1010 phase crystallized preferentially and automatically reverted to PA1010/TiC particles. As shown in the POM images (Fig. S6 in ESI), distinct crystallization features were observed at different temperatures. During heating, the crystalline morphology of PVDF gradually melted and disappeared as the temperature increased to 170 °C. As the temperature further increased to 190 °C, the PA1010 phase began to melt. During the subsequent cooling process, PA1010 and PVDF crystallized sequentially. This stepwise crystallization behavior upon cooling was also confirmed by the DSC measurements (Fig. S7 in ESI). The

post-crystallization process of PVDF generates compression and releases latent heat, which synergistically reinforces crystallization of the PA1010 phase. Compared with neat PA1010, the crystallinity of the PA1010 phase increased from 24.3% to 36.1% at a PA1010: PVDF mass ratio of 2:5, which benefitted the reconstruction of the PA1010/TiC conductive network. After cooling to room temperature, the PVDF/TiC conductive network recovered.[34,35] Notably, the participation of PA1010/TiC particles, which served as relay stations, enabled the rapid reconstruction of long-range conductive networks in the entire system. Therefore, the reproducibility of the hierarchical PPTC thermistor has been significantly improved during thermal cycling.

However, with an increase in $m_{(PA1010/TiC)}$:$m_{(PVDF/TiC)}$, the content of PA1010/TiC particles increased, and the content of PVDF/TiC particles decreased. The compression effect and heat emission from the crystallization of the PVDF phase degraded, resulting in reduced crystallinity of the PA1010 phase. Therefore, it was difficult for the PA1010/TiC conductive network to self-heal. Thus, the relay function of the PA1010/TiC particles was weakened. Thus, the reconstruction of long-range conductive networks in the entire system failed. Accordingly, the reproducibility of the hierarchical PPTC thermistor significantly decreased when the mass ratio of PA1010/TiC to PVDF/TiC was increased to 4:5. Meanwhile, if the PA1010/TiC content was relatively low, the number of relay stations was too low to build hierarchical conductive networks. Reproducibility was also unsatisfactory. Therefore, the preferred $m_{(PA1010/TiC)}$:$m_{(PVDF/TiC)}$ ratio was 2:5, and the corresponding reproducibility of the hierarchical PPTC thermistor was significantly improved during thermal cycling.

## The Stability of Hold Current of Hierarchical PPTC Thermistor

Although the *ρ-T* curve has been widely used to investigate PTC characteristics, the PTC effect of the PPTC thermistor appears under applied voltages in practical applications. It is important to note that the PTC effect caused by external heat is different from that induced by internal Joule heat, which is generated by the applied voltage. Thus, the voltage-current (*V-I*) curve of the hierarchical PPTC thermistor was studied. In a typical measurement, a thermistor was applied at a voltage between 0 and 3 V, and the hold current ($I_{hold}$) was extracted, which was defined as the maximum critical current at which the PPTC thermistor could maintain a low-resistance state. As shown in Fig. 6, with an increase in the applied voltage, the current increased linearly in the initial stage. It can be inferred that the generated Joule

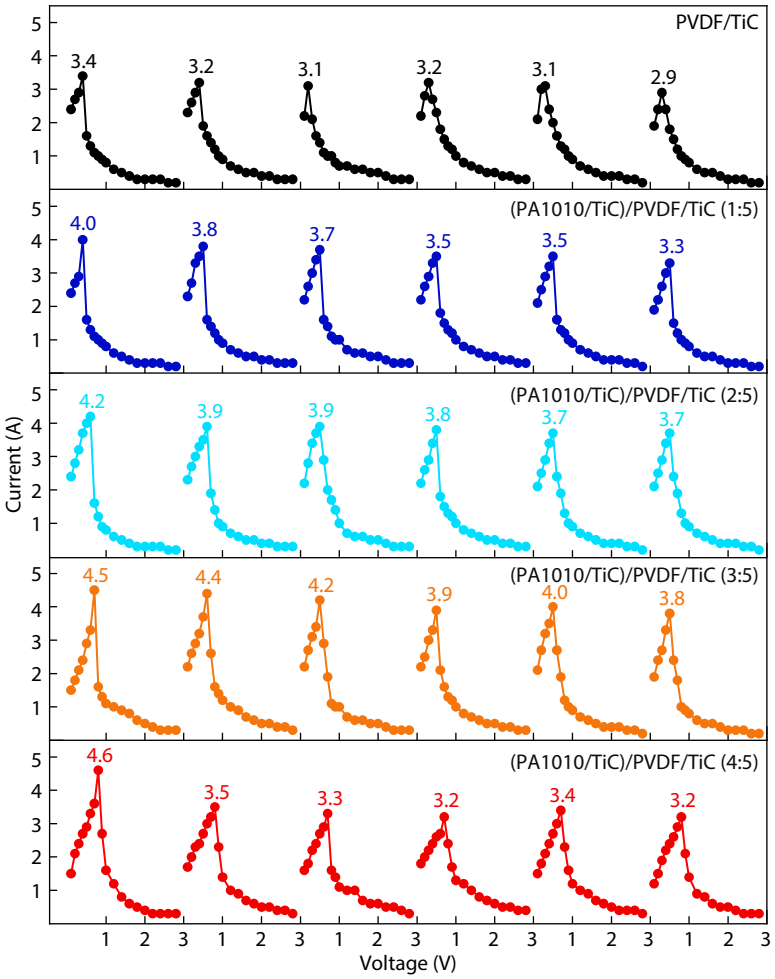


**Fig. 6** The voltage-current (*V-I*) curves and hold current ($I_{hold}$) of PVDF/TiC PPTC thermistor and the hierarchical PPTC thermistors with different $m_{(PA1010/TiC)}$:$m_{(PVDF/TiC)}$ induced by different cycling of applied voltages.

https://doi.org/10.1007/s10118-026-3658-x

heat is quickly released under a low voltage. The temperature and the resistance of the thermistor remained stable. When the current climbed to the top ($I_{hold}$), it began to decline sharply in the second stage. At this time, the generated Joule heat was significantly greater than the released heat, and the thermistor was heated to $T_s$. The resistance of the thermistor increased rapidly and overcurrent protection was triggered. Along with the decrease in current, the generated Joule heat decreased, and the rise in temperature and resistance slowed. The current decreased slowly in the third stage even when the applied voltage was further enhanced. This is the exact protection process of the PPTC thermistor.

The $I_{hold}$ of the PVDF/TiC thermistor was 3.4 A in the initial test. After six cycling tests, the $I_{hold}$ decreased to 2.9 A. There has been a decline in the stability of the $I_{hold}$. This indicates that some of the conductive networks were destroyed in the PVDF/TiC composite. When the PA1010/TiC particle was introduced, the initial $I_{hold}$ of the thermistors gradually increased to 4.6 A along with an increase in $m_{(PA1010/TiC)}$:$m_{(PVDF/TiC)}$. This is because the higher the content of the PA1010/TiC particles, the lower the resistivity of the hierarchical PPTC thermistor, which is beneficial for improving $I_{hold}$. After six cycling tests, the $I_{hold}$ of the hierarchical PPTC thermistors decreased somewhat. When the $m_{(PA1010/TiC)}$:$m_{(PVDF/TiC)}$ ratio was 1:5, $I_{hold}$ reached to 3.3 A. When the $m_{(PA1010/TiC)}$:$m_{(PVDF/TiC)}$ was further improved to 2:5 and 3:5, the $I_{hold}$ increased to 3.7 A and 3.8 A, respectively, which were significantly higher than that of PVDF/TiC thermistor (2.9 A). However, if $m_{(PA1010/TiC)}$: $m_{(PVDF/TiC)}$ increased to 4:5, $I_{hold}$ rapidly declined to 3.2 A, indicating that the stability of $I_{hold}$ degraded. This can be attributed to the fact that excessive loading of PA1010/TiC particles was detrimental to the reconstruction of the hierarchical conductive networks. These experimental results are consistent with thermal cycling research on $\rho$-$T$ curves. The minimum relative fluctuation percentages of $I_{hold}$ appeared in the hierarchical PPTC thermistor with an $m_{(PA1010/TiC)}$:$m_{(PVDF/TiC)}$ ratio of 2:5 (Table S4 in ESI). Therefore, the improved reproducibility of thermal cycling and stability of the $I_{hold}$ of the PPTC thermistor were achieved by constructing hierarchical conductive networks of (PA1010/TiC)/PVDF/TiC.

## CONCLUSIONS

Hierarchical PPTC composites of (PA1010/TiC)/PVDF/TiC were fabricated by adopting a solution-mixing strategy based on the solubility difference of polymer matrices in different solvents. The uncontrollable selective distribution of the fillers in the different polymer matrices was effectively inhibited. The hierarchical conductive networks of PVDF/TiC served as the first-level PTC material, PA1010/TiC particles acted as the other-level PTC material and relay stations were flexibly constructed. When a suitable usage of PA1010/TiC particles ($m_{(PA1010/TiC)}$:$m_{(PVDF/TiC)}$ = 2:5) was adopted, the $T_s$ and $I_{PTC}$ of the PPTC composites have been improved to 165 °C and 8.9, respectively. Furthermore, a dual PTC effect was observed, and the NTC effect was suppressed. Moreover, the reproducibility of the hierarchical PPTC thermistors was systematically investigated by studying the $\rho$-$T$ curves under thermal cycling. And the cyclic $V$-$I$ curves implying a typical PTC effect induced by the applied voltages were also studied. Benefiting from the relay function of the PA1010/TiC particles and the crystallization reinforcement effect of PVDF, the rapid reconstruction of long-range conductive networks in the entire system was achieved. Thus, the reproducibility and $I_{hold}$ of the hierarchical PPTC thermistor are significantly improved. This work provides new insights into the design and manufacture of dual-matrix PPTC thermistors, which would be of great significance for improving their performance.

## Conflict of Interests

The authors declare no interest conflict.

## Electronic Supplementary Information

Electronic supplementary information (ESI) is available free of charge in the online version of this article at http://doi.org/10.1007/s10118-026-3658-x.

## Data Availability Statement

The data supporting the findings of this study are available from the corresponding author upon reasonable request.

## ACKNOWLEDGMENTS

This work was financially supported by the Undergraduate Training Program on Innovation and Entrepreneurship (Nos. 202510251118S and 202510251085).

## REFERENCES

1 Go, G. M.; Park, S.; Lim, M.; Jang, B.; Park, J. Y.; Cho, H. B.; Choa, Y. H. Enhanced positive temperature coefficient intensity and reproducibility with synergistic effect of 0-D and 2-D filler composites. *J. Mater. Sci.* **2022**, *57*, 18037–18050.
2 Wang, Y. F.; Chen, X. Y. Investigation of the positive temperature coefficient resistivity of Nb-Doped $Ba_{0.55}Sr_{0.45}TiO_3$ ceramics. *Crystals.* **2024**, *14*, 419.
3 Chen, P.; Lu, Z. K.; Ji, L. M.; Li, Y. F. Design of the control scheme of power battery low-temperature charging heating based on real-vehicle applications. *IEEE Veh. Power Propuls. Conf. (VPPC)* **2013**, 105–110.
4 Gao, C.; Fu, Q. Y.; Zhou, D. X.; Zu, H.; Chen, T.; Xue, F.; Hu, Y. X.; Zheng, Z. P.; Luo, W. Nanocrystalline semiconducting donor-doped $BaTiO_3$ ceramics for laminated PTC thermistor. *J. Eur. Ceram. Soc.* **2017**, *37*, 1523–1528.
5 Safonov, E.; Frolov, V.; Zhiligotov, R.; Petrenya, Y. The specifics of PTC thermistor applications for limiting surge currents. *Energies* **2024**, *17*, 318.
6 Yu, A. M.; Li, Q. Study on thermal control behavior using $BaTiO_3$-based PTC materials with room-temperature Curie point. *ASME Int. Conf. Micro/Nanoscale Heat Mass Transfer* **2019**, *58905*, V001T06A001.
7 Shin, Y. H.; Sim, S.; Kim, S. C. Performance characteristics of a modularized and integrated PTC heating system for an electric vehicle. *Energies* **2016**, *9*, 18.
8 Cicek, U. I.; Southee, D. J.; Johnson, A. A. The development and characterisation of 3D-printed multi-material thermistor. *Addit.*

## Graphical Abstract

### Facile Construction of Hierarchical Polymeric Positive Temperature Coefficient Composites for Improved Reproducibility

Bao-Yu Wang, Heng-Yu Zhao, Xin Ji, Wei Hu, Yu-Ru Duan, Jian-Ze Li, Zi-Hao Zhang, Ying Liang, Bin Fang, and Zhen Zhang

*East China University of Science and Technology*

A solution-mixing strategy based on the solubility difference of polymers was employed to fabricate hierarchical polymeric positive temperature coefficient (PPTC) composites. Benefiting from the relay function of the PA1010/TiC particles, the reproducibility was significantly improved.

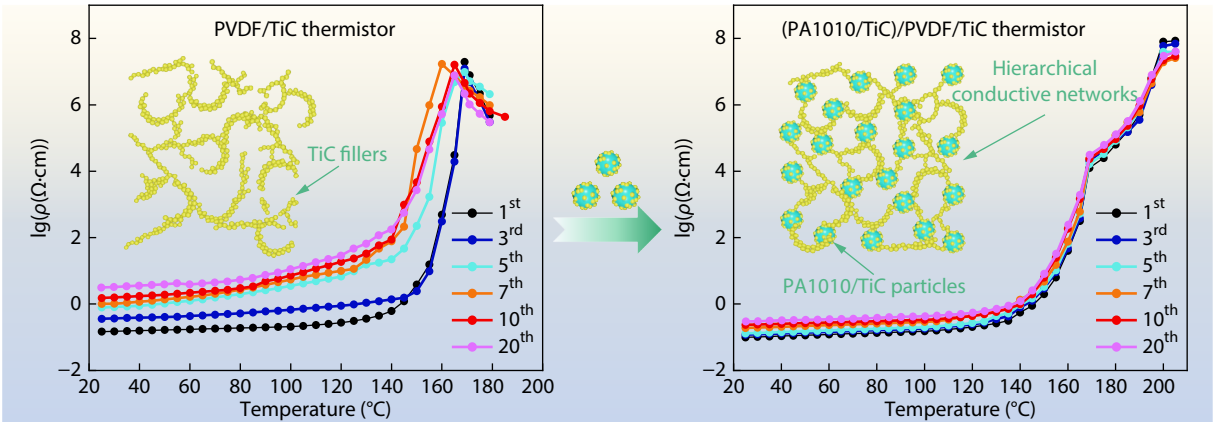


*Chinese J. Polym. Sci. 2026, 44, 2681–2690* *https://doi.org/10.1007/s10118-026-3658-x*

*Manuf.* **2024**, *94*, 104510.

9 Cao, S. Y.; Shi, C. Y.; Kong, F.; Liu, Y.; Fan, Y. W.; Tuo, Y. L.; Wang, J. H.; Yao, J. C.; Chang, A. M. Fabrication and properties of fast-response NTC chip thermistors based on Mn-Co-Fe-Mg-M-O (M=Zn, Cr) high-entropy ceramics. *Mater. Sci. Semicond. Process.* **2025**, *189*, 109278.

10 Ouni, I.; Moualhi, Y.; Rahmouni, H. Thermistor and capacitor parameter analysis through electrical and dielectric investigations of manganite systems for technological applications. *Sensor Actuat A-Phys.* **2025**, *384*, 116300.

11 Ding, S. W.; Pan, B.; Jia, G.; Li, L. F. Influence of Bi and Nb codoping on the behaviors of $BaTiO_3$-based PTC ceramics. *Chin. J. Inorg. Chem.* **2012**, *28*, 40–44.

12 Huang, H.; Chen, Y.; Li, Z.; Yang, H.; Yang, Z.; Guo, J. C.; Yang, Y. The influences of controlling sintering mechanism on electrical properties of multilayer PTCR chip. *J. Wuhan Univ. Technol.-Mater. Sci. Ed.* **2015**, *30*, 674–678.

13 Chen, Y.; Gong, S. P.; Zhang, B.; Cao, W. Q.; Yu, D. P.; Liu, Z. Y.; Wang, W. F. The preparation of fine-grained positive temperature coefficient resistance with superior electrical properties. *Microelectron. Eng.* **2013**, *103*, 106–110.

14 Zha, J. W.; Wu, D. H.; Yang, Y.; Wu, Y. H.; Li, R. K. Y.; Dang, Z. M. Enhanced positive temperature coefficient behavior of the high-density polyethylene composites with multi-dimensional carbon fillers and their use for temperature-sensing resistors. *RSC Adv.* **2017**, *7*, 11338–11344.

15 Liu, K.; Xu, Z.; Mei, J.; Han, J. L.; Zheng, F. H.; Wang, H. Q.; Huang, Y. G.; Wu, Q.; Qin, G. F.; Jiang, J. T.; Li, Q. Y. Strategies for improving positive temperature effects in conductive polymer composites: A review. *J. Mater. Chem. C* **2023**, *11*, 4966–4992.

16 Cheng, W. L.; Yuan, S.; Song, J. L. Studies on preparation and adaptive thermal control performance of novel PTC materials with controllable Curie temperatures. *Energy* **2014**, *74*, 447–454.

17 Bakhtiar, S. U. H.; Dong, T. W.; Xue, B. X.; Ali, S.; Sattar, H.; Dong, W.; Fu, Q. Y. Positive temperature coefficient materials for intelligent overload protection in the new energy era. *Mater. Today* **2023**, *71*, 108–134.

18 Tang, Q. Z.; Fan, S. C.; Yang, Y.; Hu, W.; Qian, C.; Ji, X.; Zhang, Z.; Liang, Y.; Fang, B. Effect of gradient distribution of fillers on polymeric PTC thermistors prepared by solution mixing and subsiding method. *Compos. Commun.* **2023**, *42*, 101661.

19 Chen, L.; Zhang, J. M. Designs of conductive polymer composites with exceptional reproducibility of positive temperature coefficient effect: A review. *J. Appl. Polym. Sci.* **2021**, *138*, 49677.

20 Okutani, C.; Yokota, T.; Matsukawa, R.; Someya, T. Suppressing the negative temperature coefficient effect of resistance in polymer composites with positive temperature coefficients of resistance by coating with parylene. *J. Mater. Chem. C* **2020**, *8*, 7304–7308.

21 Jiang, G. M.; Zhou, Y. X.; Teng, C. Y.; Zhang, Y. X.; Huang, X.; Xue, L.; Zhou, L. M. Electrical resistivity-temperature characteristics enhancement of insulating cross-linked polyethylene composites by incorporating positive temperature coefficient particles with different Curie temperatures. *High Volt.* **2023**, *8*, 1–11.

22 Deng, H.; Skipa, T.; Zhang, R.; Lellinger, D.; Bilotti, E.; Alig, I.; Peijs, T. Effect of melting and crystallization on the conductive network in conductive polymer composites. *Polymer* **2009**, *50*,

3747–3754.
23 Pang, H.; Xu, L.; Yan, D. X.; Li, Z. M. Conductive polymer composites with segregated structures. *Prog. Polym. Sci.* **2014**, *39*, 1908–1933.
24 Chen, L.; Wu, X.; Zhang, X. F.; Zhang, J. M. Enhanced reproducibility of positive temperature coefficient effect of CB/HDPE/PVDF composites with the addition of ionic liquid. *Chinese J. Polym. Sci.* **2021**, *39*, 228–236.
25 Liu, G. S.; Zhao, Y. S.; Lin, M. J.; Zhang, L.; Li, G. X.; Liao, X. Preparation of controllable and repeatable crystalline states through step-by-step self-nucleation programming and its application for improving the PTC reproducibility of trans-1,4-polyisoprene/carbon black composites. *Ind. Eng. Chem. Res.* **2024**, *63*, 9800–9810.
26 Lu, C.; Hu, X. N.; He, Y. X.; Huang, X. H.; Liu, J. C.; Zhang, Y. Q. Triple percolation behavior and positive temperature coefficient effect of conductive polymer composites with especial interface morphology. *Polym. Bull.* **2012**, *68*, 2071–2087.
27 Wei, Y.; Li, Z. Y.; Liu, X. H.; Dai, K.; Zheng, G. Q.; Liu, C. T.; Chen, J. B.; Shen, C. Y. Temperature-resistivity characteristics of a segregated conductive CB/PP/UHMWPE composite. *Colloid Polym. Sci.* **2014**, *292*, 2891–2898.
28 Kim, C. H.; Lee, S. Y.; Park, S. J. Positive/negative temperature coefficient behaviors of electron beam-irradiated carbon blacks-loaded polyethylene nanocomposites. *ACS Omega* **2022**, *7*, 47933–47940.
29 Zhang, X.; Zheng, S. D.; Zou, H. Z.; Zheng, X. F.; Liu, Z. Y.; Yang, W.; Yang, M. B. Two-step positive temperature coefficient effect with favorable reproducibility achieved by specific "island-bridge" electrical conductive networks in HDPE/PVDF/CNF composite. *Compos. Part A Appl. Sci. Manuf.* **2017**, *94*, 21–31.
30 Liu, J. Y.; Chen, C. M.; Tao, Y.; Zhang, J.; Huang, Z. H.; Luo, X.; Liu, R. H.; Ye, L. J.; Li, Y. J. Building efficient 3D networks by controlled localization of hybrid fillers in immiscible polymer blends. *ACS Appl. Polym. Mater.* **2024**, *6*, 5366–5373.
31 Göldel, A.; Marmur, A.; Kasaliwal, G. R.; Pötschke, P.; Heinrich, G. Shape-dependent localization of carbon nanotubes and carbon black in an immiscible polymer blend during melt mixing. *Macromolecules* **2011**, *44*, 6094–6102.
32 Baudouin, A. C.; Devaux, J.; Bailly, C. Localization of carbon nanotubes at the interface in blends of polyamide and ethylene-acrylate copolymer. *Polymer* **2010**, *51*, 1341–1354.
33 Bao, Y.; Xu, L.; Pang, H.; Yan, D. X.; Chen, C.; Zhang, W. Q.; Tang, J. H.; Li, Z. M. Preparation and properties of carbon black/polymer composites with segregated and double-percolated network structures. *J. Mater. Sci.* **2013**, *48*, 4892–4898.
34 Stalmann, G.; Matic, A.; Jacobsson, P.; Tranchida, D.; Gitsas, A.; Gkourmpis, T. Crystallisation kinetics and associated electrical conductivity dynamics of poly(ethylene vinyl acetate) nanocomposites in the melt state. *Nanomaterials* **2022**, *12*, 3602.
35 Setnescu, R.; Lungulescu, E. M.; Marinescu, V. E. Polymer composites with self-regulating temperature behavior: Properties and characterization. *Materials* **2022**, *16*, 157.

https://doi.org/10.1007/s10118-026-3658-x